Microwave-induced dc voltages in a $YBa_2Cu_3O_{7-\delta}$ single crystal

D. C. Ling,* J. T. Chen, and L. E. Wenger

Department of Physics and Astronomy, Wayne State University, Detroit, Michigan 48202

(Received 15 December 1995)

Microwave-induced dc voltages in a $YBa_2Cu_3O_{7-\delta}$ single crystal have been observed along its c axis with or without a dc bias current by utilizing standing waves near the end of an X-band (8–12 GHz) waveguide. With a dc bias current present, the induced voltages arise from both bolometric and nonbolometric effects; however, the characteristics of the induced voltages versus bias currents due to these two effects are distinctively different. In the bolometric effect, the induced voltages are simply due to a resistive change caused by microwave heating whereas the induced voltages from the nonbolometric effect are due to the Josephson vortex flow generated by the microwave H field below the superconducting transition temperature. Without a dc bias current, the induced voltages are attributed to the inverse ac Josephson effect which requires the presence of both the microwave E and H fields. [S0163-1829(96)03422-4]

To date, it is generally believed that the high-T_c superconductivity is intrinsically two-dimensional[1–4] in the CuO_2 bilayers or trilayers coupled together by the Josephson currents along the c axis. Kleiner and co-workers[5,6] have investigated the coupling between CuO_2 layers in $YBa_2Cu_3O_{7-\delta}$ (YBCO), $Bi_2Sr_2CaCu_2O_8$ (BSCCO) and $Tl_2Ba_2Ca_2Cu_3O_{10}$ (TBCCO) single crystals by direct measurements of the dc and ac Josephson effects with currents flowing in the c-axis direction. They found that the I-V characteristics of BSCCO and TBCCO exhibit large hystereses and multiple branches indicative of a stack of Josephson junctions connected in series. For BSCCO and TBCCO, the oscillations in the critical current as a function of magnetic field (parallel to the layers) indicate that these intrinsic Josephson junctions probably exist between the CuO_2 bilayers or trilayers of neighboring unit cells along the c axis of the single-crystal sample. However, similar experimental evidence for intrinsic Josephson junctions in a YBCO single crystal was not found in simple I-V measurements. This may be due to the stronger coupling between the CuO_2 layers in YBCO owing to the more metalliclike nature of the materials coupling the CuO_2 layers and thus giving rise to a superconducting–normal-metal–superconducting type of junction with a smaller ρ_c. Moreover, experiments on high-quality Josephson junctions composed of a conventional superconductor Pb and a single crystal of YBCO suggest that there is no energy gap for YBCO along the c axis.[7] This absence of an energy gap together with the smaller ρ_c makes it more difficult to observe an intrinsic Josephson effect in YBCO by I-V measurements. More recently, measurements of the dynamic resistance versus magnetic field utilizing a modulation technique on a YBCO single crystal along the c axis indicate not only the existence of inter-unit-cell Josephson junctions in YBCO but also of intra-unit-cell Josephson junctions formed by the CuO_2-Y-CuO_2 atomic planes themselves.[8]

Previously, some unusual microwave effects indicating the presence of Josephson junctions in films and ceramic samples of the high-T_c cuprate superconductors have been observed.[9–12] For these experiments, it is not clear whether the observed effects originated from intergrain, intragrain, or unit-cell junctions. Thus, investigating microwave responses in a single-crystal sample may yield more definitive information about the source of the junctions. In this article, we present results from our study of microwave-induced dc voltages on a YBCO single crystal along the c axis as a function of frequency, sample position, and bias current. This experiment elucidates our understanding of how microwaves are coupled to a YBCO single crystal and the roles that the microwave E and H fields have in inducing the dc voltages.

$YBa_2Cu_3O_{7-\delta}$ single crystals with dimensions of 1 mm$\times$1 mm$\times$50 μm were grown by a self-flux growth method using a 1:37:90 mixture of Y_2O_3, BaO_2, and CuO powders.[13] X-ray-diffraction data showed that the crystals were c-axis oriented with a c-axis lattice spacing of 11.7 Å. In order to have a more uniform current distribution and to ensure the two voltage contacts at the same equipotential levels as the two current contacts, two silver layers with thickness of 1 μm were deposited by e-beam evaporation over the entire opposite surfaces (parallel to the ab planes) of the single crystal. Four electrical contacts were made by attaching gold wires to the silver layers with silver epoxy and then curing in O_2 at 500 °C for 5 h, with the typical contact resistance being on the order of 0.1 Ω. The temperature dependences of resistivity have the usual behaviors, namely linear for ρ_{ab} vs T and an inverse temperature dependence for ρ_c vs T. The onset temperatures of the superconducting transition along the c axis are typically in the range of 84–89 K.

A YBCO single-crystal sample is mounted near the end of an X-band (8–12 GHz) waveguide such that the microwave H field is in the ab planes and the E field parallel to the c axis of the single-crystal sample. By moving the sliding short near the end of the waveguide, the relative position of the sample can be effectively changed with respect to the maxima of the E and H fields of the microwave. Since the maxima of the E and H fields of the microwave are separated by one quarter of wavelength near the end of the waveguide, the single-crystal sample can be coupled to the E or H fields of the microwave selectively by moving the sliding short. A μ-metal shield is placed around the outside of the nitrogen dewar to shield the sample from earth's magnetic field as well as any other stray fields. All electrical leads near the sample are firmly taped down to prevent any mechanical
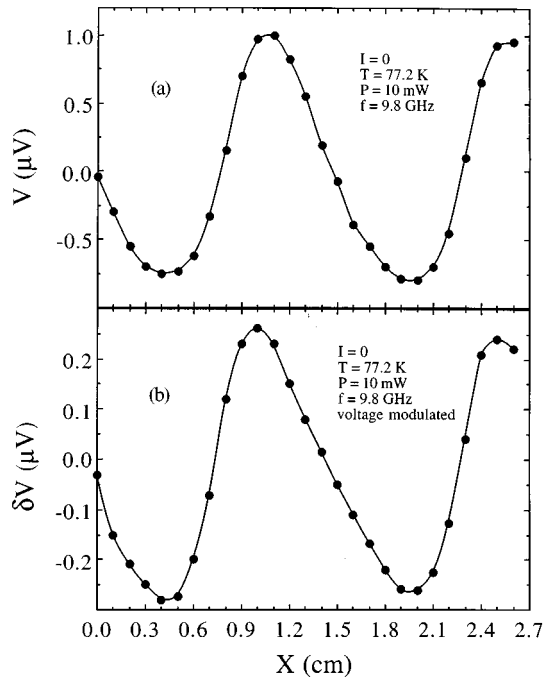
FIG. 1. (a) Microwave-induced dc voltage versus sample position in an X-band waveguide. The dc voltage is measured along the c axis of a YBCO single crystal without a bias current. (b) Similar results obtained by using a microwave amplitude modulation technique and measuring the phase-sensitive voltage δV.
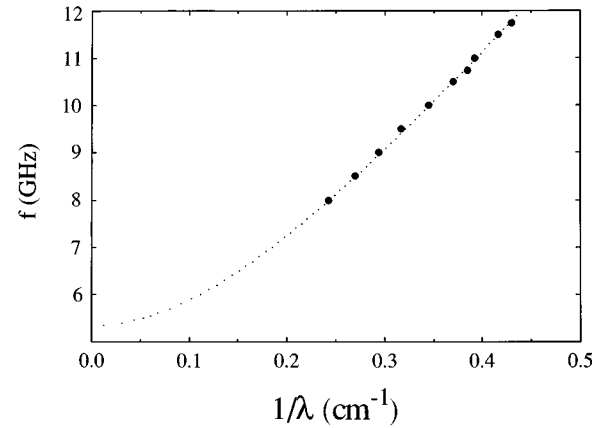

FIG. 2. The dispersion relation of the X-band waveguide in liquid oxygen. The closed circles are experimental data and the dotted line is based on a theoretical calculation of the dispersion relation for a rectangular waveguide.

vibration. In addition, each pair of electrical leads are twisted and properly arranged to minimize any inductive pickup. Microwave-induced dc voltages in the single crystal are then measured along its c axis with or without a dc bias current. Since the induced dc voltage is typically on the order of a μV or less, which is not much more than the noise level of the nanovoltmeter ($\sim$20 nV) and comparable to the thermal drift voltage, a phase-sensitive modulation technique is employed. In this technique, the microwave power is modulated electrically by simply applying an ac voltage across the modulator inserted in series with the microwave oscillator and the waveguide and the induced voltages are detected at a modulation frequency by using a lock-in amplifier. This technique allows us to detect an effect as small as 0.2 nV, two orders of magnitude more sensitive than the direct dc measurements. The other advantage of this technique is to remove the background dc voltage arising from the normal-state resistance in a biased case so that only the effect due to microwaves will be measured.

An example of the microwave-induced voltage as a function of sample position with respect to the end of the waveguide is shown in Fig. 1. In Fig. 1(a), the induced dc voltage measured across an unbiased YBCO single crystal in the c-axis direction as function of the sample position clearly shows a standing wave pattern with both positive and negative polarities. This polarity reversibility rules out simple rectification as a possible explanation. The phase-sensitive detected voltage signal from the modulation technique corresponding to a 30% amplitude modulation is shown in Fig. 1(b) for comparison. It is clearly evident that there is both qualitative as well as quantitative correlation between the voltage signals of Figs. 1(b) and 1(a).

Figure 1 also shows that the distance between the two adjacent peaks is about 1.5 cm. By taking into account the dielectric constant of liquid nitrogen and the dispersion relation of the waveguide, the wavelength of the microwave in the X-band waveguide is calculated to be 3.05 cm at 9.8 GHz. This observed spatial period of the induced voltage being only one-half of the microwave wavelength in combination with the appearance of both positive and negative polarities suggests that the pattern is related to the product of the microwave E and H fields as will be discussed more fully later. To see if the patterns of the induced voltages are indeed medium related, we have performed the experiments with the sample in liquid oxygen, in nitrogen gas, and in oxygen gas. In each case, the spacings between the two adjacent peaks are one-half of the wavelength and the spacings vary according to the changes in the dielectric constants. An example of the dispersion relation in liquid oxygen with a doubling of the spacing is shown in Fig. 2. Note the good agreement to the theoretical formula for the dispersion relation of an X-band rectangular waveguide, $\kappa = [\omega^2 - \omega_c^2]^{1/2} \varepsilon^{1/2}/c$, where ω_c is the cutoff angular frequency of the waveguide, κ is the wave vector, and ε is the dielectric constant.

A typical microwave-induced voltage-versus-frequency spectrum in the absence of a bias current is shown in Fig. 3. The data clearly exhibit an oscillatory behavior including both positive and negative polarities with the bar representation of the data indicating the range of the variation in the induced voltage as the relative sample position is changed. The observed polarity reversal and oscillatory behavior rule out an artifact such as rectification or differential heating arising from any nonuniformity in the sample as a source of the microwave-induced voltages. On the other hand, the observed oscillatory and polarity reversal properties of the induced voltages as a function of microwave frequency and power are qualitatively consistent with the inverse ac Josephson effect in which the induced dc voltage is related to the Bessel function behavior.[14]

To indeed verify that these microwave-induced voltages are associated with the presence of superconductivity, Fig. 4 shows the temperature dependence of the microwave-
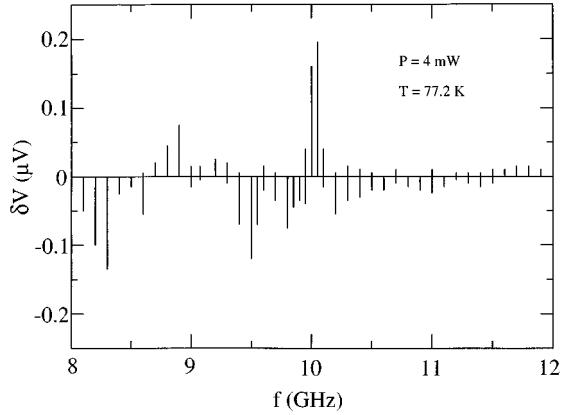
FIG. 3. Microwave-induced dc voltage δV versus frequency spectrum for an unbiased YBCO single crystal along the c axis. The bar represents the range of the variation in the induced voltage as the relative sample position is changed. (See Fig. 1.)

induced voltage δV for an unbiased YBCO single crystal ($T_{\text{onset}}=89$ K from resistivity measurements) along the c axis. The onset of an appreciable microwave-induced voltage occurs at 90 K, the same temperature as the onset temperature of the $YBa_2Cu_3O_{7-\delta}$ superconducting phase, indicating that the induced voltage must be associated with its superconducting transition. To further elucidate the nature of the microwave-induced voltages, the bias current dependences were studied as a function of microwave power and temperature. As can be seen in Fig. 5, there appears to be a distinct difference between the induced voltage behaviors below and above the superconducting transition temperature. For $T>T_c$, the induced dc voltages δV versus bias current are simply linear at all levels of microwave power as shown in Fig. 5(a). The negative slopes as well as the power dependence can be easily understood in terms of simple heating or
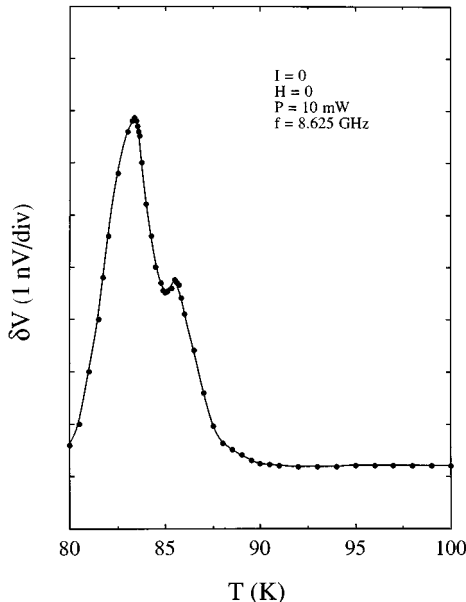

FIG. 4. The temperature dependence of the microwave-induced dc voltage δV along the c axis for an unbiased YBCO single crystal.
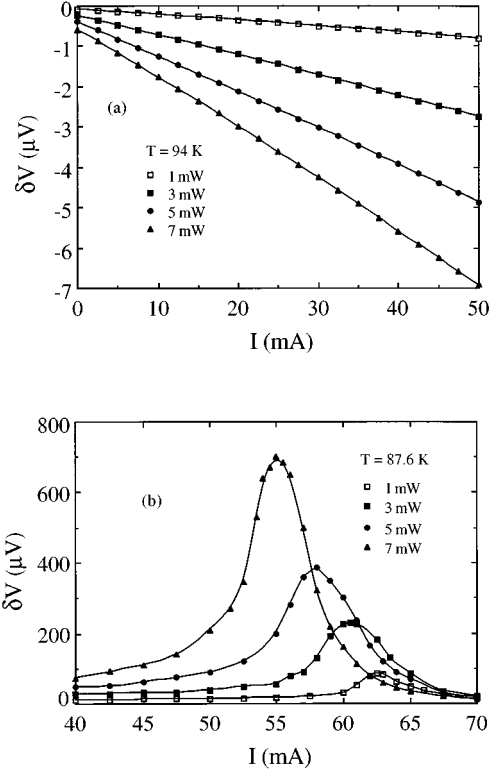

FIG. 5. (a) Microwave-induced dc voltage δV versus bias current for various values of incident microwave power at a temperature above T_c. (b) Microwave-induced dc voltage δV versus bias current for various values of incident microwave power at a temperature below T_c.

a bolometric effect. Recall that the temperature dependence of the resistance in the c-axis direction is inversely proportional to the temperature, i.e., $R \propto 1/T$. If the microwave absorption by a normal metal causes a simple heating of $\delta T \propto \delta P$, one expects $\delta R = (dR/dT)\delta T$ to result in an induced voltage of

$$\delta V = I\delta R = I(dR/dT)\delta T \propto -I(1/T^2)\delta P, \quad (1)$$

which predicts a power-dependent negative slope in the δV vs I plot. This is exactly the behavior observed in Fig. 5(a). Although this bolometric effect can persist below T_c, the induced dc voltages versus bias current shown in Fig. 5(b) have a totally different behavior as well as being one-to-two orders of magnitude larger. The microwave-induced voltage δV exhibits a peak which shifts towards lower current values and increases in height as the microwave power increases. The current values corresponding to the positions of these δV peaks compare favorably to the critical current I_0 as determined from the I-V characteristics of the sample for similar microwave powers suggesting that these induced voltages δV vs I can be qualitatively understood as follows. If the microwaves cause a small reduction in the critical current, it leads to an increment in the voltage given approximately by

$$\delta V = (dV(I)/dI)\delta I_0(P), \quad (2)$$

where $dV(I)/dI$ is the dynamic resistance at I and $\delta I_0(P)$ is the reduction in I_0 caused by microwaves of power P. The peak structure arises from the maximum in $dV(I)/dI$ at $I \approx I_0$
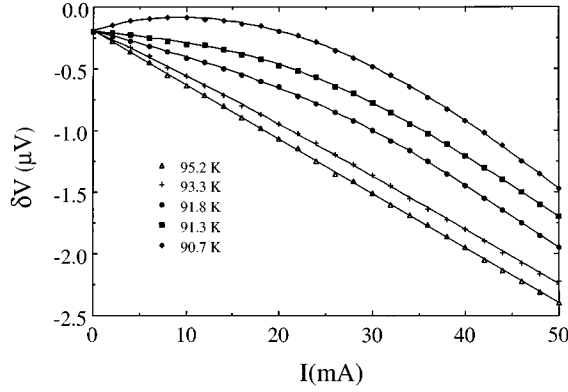
FIG. 6. Microwave-induced dc voltage δV versus bias current for several temperatures near T_c.

FIG. 7. Microwave-induced dc voltage δV versus sample position for various bias currents along the c axis of a YBCO single crystal.

and the power dependence comes from $\delta I_0(P)$. Thus, the microwave-induced dc voltages in a YBCO single crystal along the c axis can be described by two terms,

$$\delta V = (dV/dI)\delta I_0 + I(dR/dT)\delta T. \qquad (3)$$

The first term dominates when the sample is in the superconducting state where δI_0 is microwave power dependent and dV/dI has a peak structure at $I \approx I_0$. The second term is simply related to the resistance change caused by heating. Since the two terms have contrasting behaviors as demonstrated in Figs. 5(a) and 5(b), a simple δV versus I experiment with microwave radiation can be used to determine whether a sharp resistance transition is associated with the occurrence of a superconducting transition or not. For example, a set of δV versus I curves for temperature near T_c are shown in Fig. 6. One sees that for $T=95.2$ K, the δV versus I is a straight line. As the temperature is lower, nonlinearity occurs and a broad peak develops at 90.7 K. The onset temperature of superconductivity can be estimated to be 93 K, slightly higher than the 90 K determined from the corresponding resistance measurement.

In order to further our understanding of the nature of the coupling giving rise to the microwave-induced dc voltages in the superconducting state, a more detailed study of the sample position dependence of the induced voltages at different bias current levels was undertaken. Without a bias current, the peak positions of the standing wave pattern are clearly not correlated with either the maxima of the microwave E field nor the H field alone as previously shown in Fig. 1. However, in the presence of a bias current, the peak positions, within experimental uncertainty, seem to shift toward the maxima of the microwave H field with increasing current as evidence in Fig. 7. Figure 7 also shows that the peak heights increase in the direction of the bias current. Thus the direction of the bias current appears to govern the polarity of the induced voltages as seen more clearly in the high bias current regime of Fig. 8, which indicates that the entire voltage pattern under these experimental conditions can have the same sign as the current.

It should be noted that microwaves cannot induce a dc voltage in a conventional bulk superconductor without an external dc bias current. Even with a bias current, an external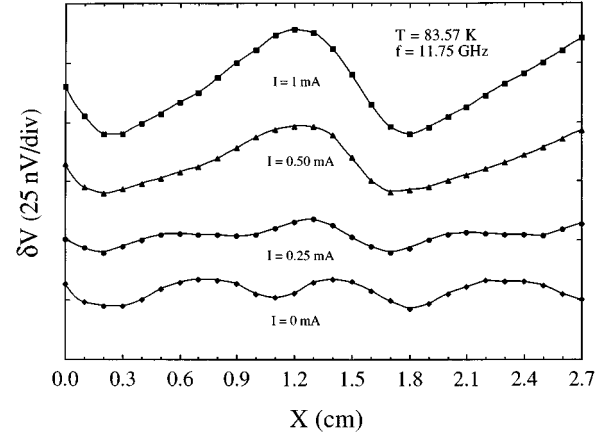 magnetic field is required for inducing a dc voltage associated with the flow of Abrikosov vortices. One possible explanation for the observed induced voltages in the YBCO single crystals for $T<T_c$ is that there are Josephson junctions within the single-crystal sample. The fact that microwaves can induce a dc voltage in a Josephson junction in the absence of both a bias current and an external magnetic field has been previously established.[14] For a Josephson junction which has a spatially uniform phase (short junction without a magnetic field present), microwave radiation of frequency f can produce quantized dc voltages, $V=nhf/2e$, known as Shapiro steps, even when a junction is not biased by an external current. If the phase of a Josephson junction is not uniform (e.g., due to an external magnetic field, a self-generated magnetic field associated with the current, or another source of spatial nonuniformity), the induced dc voltage need not be quantized. Based on the Josephson relation, the induced voltage in this case arises from the phase propagation given by

$$V = \hbar\dot\phi/2e = (\hbar/2e)(\partial\phi/\partial x)(\partial x/\partial t), \qquad (4)$$

where $(\partial\phi/\partial x)$ is related to the total internal magnetic field and $(\partial x/\partial t)$ is the phase speed determined by the Lorentz force on a Josephson vortex.
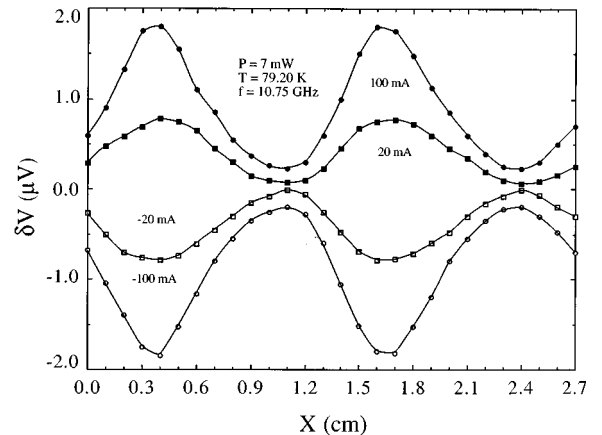

FIG. 8. Microwave-induced dc voltage δV versus sample position in a high-current regime.

Let us consider the situation where the sample is coupled to the microwave H field and there is a bias current. If the amplitude H_0 of the microwave H field exceeds a threshold for generating a flux quantum, Josephson vortices/antivortices can be generated in the junction.[15] In the presence of a bias current, these vortices/antivortices experience a Lorentz force causing them to propagate in opposite directions and produce a dc voltage which has the same polarity as the bias current I. Qualitatively speaking, since $\partial\phi/\partial x \propto |H_0|$ and $\partial x/\partial t \propto I$, then $V \propto |H_0|I$. This qualitatively describes the observed patterns shown in Figs. 7 and 8 where the induced voltages have maxima near the maxima of the H fields and the polarity of the induced voltage is the same as that of the bias current.

If no bias current is present, the vortices generated by the microwave H field cannot propagate without also being coupled to the microwave E field because of the lack of a Lorentz force. When a microwave E field is present, an internal current within the junction can be generated according to $\mathbf{J}=\sigma\mathbf{E}$, which in turn can produce a Lorentz force in the direction of $\mathbf{J}\times\mathbf{H}$ or $\mathbf{E}\times\mathbf{H}$, where σ is the quasiparticle tunneling conductivity of the sample. Although $\mathbf{E}$ and $\mathbf{H}$ are in-phase in free space, there can be a phase difference between the E and H fields in a Josephson junction because of the different Josephson phase relationships for the E and the H fields. Assuming that $E=E_0 \sin(2\pi x/L+\theta)\sin(\omega t)$ and $H=H_0\cos(2\pi x/L)\sin(\omega t)$, the induced dc voltage has the form of

$$V\propto E_0 H_0\sin(2\pi x/L+\theta)\cos(2\pi x/L). \qquad (5)$$

The actual pattern would then depend on the phase θ with the maxima separated by one-half wavelength. For example, the standing wave pattern could have both positive and negative polarities as the position X is varied or even be entirely negative or positive for $\theta=\pm\pi/2$.

In summary, we have studied microwave induced dc voltages in a $YBa_2Cu_3O_{7-\delta}$ single crystal along its c axis with or without a dc bias current by utilizing standing waves near the end of an X-band (8–12 GHz) waveguide. It has been found experimentally that bolometric and nonbolometric effects are responsible for the induced voltages in a current-biased case. While the bolometric effect results in a simple linear behavior due to a resistive change, the nonbolometric effect gives rise to nonlinear induced voltages which are due to the Josephson vortex flow generated by the microwave H field below the superconducting transition temperature. Thus a simple microwave-induced voltage versus bias current plot can be used to distinguish between the two effects and to determine whether a sharp resistance transition is superconducting in nature. In the absence of a dc bias current, the induced voltages are attributed to a self-excitation mode, which requires the presence of both the E and H fields of the microwave. The observed phenomena have confirmed a recent suggestion[8] that intrinsic Josephson junctions exist in YBCO single crystals.

*Present address: Materials Research Center, National Tsing Hua University, Hsinchu, Taiwan.

[1] R. D. Harshman and A. P. Mills, Jr., Phys. Rev. B **45**, 10 684 (1992); and references therein.

[2] N. E. Bickers, D. J. Scalapino, and S. R. White, Phys. Rev. Lett. **62**, 961 (1989).

[3] P. Monthoux, A. Balatsky, and D. Pines, Phys. Rev. B **46**, 14 803 (1992).

[4] S. Chakravarty, A. Sudbø, P. W. Anderson, and S. Strong, Science **261**, 337 (1993).

[5] R. Kleiner, F. Steinmeyer, G. Kunkel, and P. Müller, Phys. Rev. Lett. **68**, 2394 (1992); R. Kleiner and P. Müller, Phys. Rev. B **49**, 1327 (1994).

[6] R. Kleiner, P. Müller, H. Kohlstedt, N. F. Pedersen, and S. Sakai, Phys. Rev. B **50**, 3942 (1994).

[7] A. G. Sun, D. A. Gajewski, M. B. Maple, and R. C. Dynes, Phys. Rev. Lett. **72**, 2267 (1994); A. G. Sun, L. M. Paulius, D. A. Gajewski, M. B. Maple, and R. C. Dynes, Phys. Rev. B **50**, 3266 (1994).

[8] D. C. Ling, G. Yong, J. T. Chen, and L. E. Wenger, Phys. Rev. Lett. **75**, 2011 (1995).

[9] J. T. Chen, L. E. Wenger, C. J. McEwan, and E. M. Logothetis, Phys. Rev. Lett. **58**, 1972 (1987).

[10] K. Chang, J. T. Chen, L. E. Wenger, and E. M. Logothetis, Physica C **162**–**164**, 1591 (1989).

[11] K. Chang, G. Yong, L. E. Wenger, and J. T. Chen, J. Appl. Phys. **69**, 7316 (1991).

[12] B. G. Boone, R. M. Sova, K. Moorjani, and W. J. Green, J. Appl. Phys. **69**, 2676 (1991).

[13] R. Boutellier, B. N. Sun, H. J. Sheel, and H. Schmid, J. Cryst. Growth **96**, 465 (1989).

[14] J. T. Chen, R. J. Todd, and Y. W. Kim, Phys. Rev. B **5**, 1843 (1972).

[15] T. V. Rajeevakumar, J. X. Przybysz, and J. T. Chen, Solid State Commun. **25**, 767 (1978).